FEBS Letters 589 (2015) 1067–1071

journal homepage: www.FEBSLetters.org

Photochemical chromophore isomerization in histidine kinase rhodopsin HKR1

Meike Luck [a,1], Sara Bruun [b,1], Anke Keidel [b], Peter Hegemann [a,*], Peter Hildebrandt [b,*]

[a] Humboldt Universität zu Berlin, Institut für Biologie, Experimentelle Biophysik, Invalidenstr. 42, D-10115 Berlin, Germany
[b] Technische Universität Berlin, Institut für Chemie, Sekr. PC14, Straße des 17. Juni 135, D-10623 Berlin, Germany

ARTICLE INFO

Article history:
Received 5 March 2015
Accepted 20 March 2015
Available online 31 March 2015

Edited by Richard Cogdell

Keywords:
Microbial rhodopsin
Histidine kinase
Isomerization
Resonance Raman
Photoswitch

ABSTRACT

Histidine kinase rhodopsin 1 is a photoreceptor in green algae functioning as a UV-light sensor. It switches between a UV-absorbing state (Rh-UV) and a blue-absorbing state (Rh-Bl) with a protonated retinal Schiff base (RSB) cofactor in a mixture of 13-*trans*,15-*anti* and 13-*cis*,15-*syn* isomers. The present spectroscopic study now shows that cofactor-protein assembly stabilizes the protonated 13-*trans*,15-*anti* RSB isomer. Formation of the active photoswitch requires the photoinduced conversion to Rh-UV. The transitions between the Rh-Bl isomers and the deprotonated 13-*cis*,15-*anti* and 13-*trans*,15-*syn* isomers of Rh-UV proceed via multiple photoisomerizations of one or simultaneously two double bonds.

1. Introduction

Microbial rhodopsins are widespread photoreceptors in prokaryotes and lower eukaryotic groups [1]. They utilize light as a source of energy or information to drive ATP synthesis or to trigger physiological responses. Among them, the well-studied bacteriorhodopsin (BR) that serves as a light-driven proton pump was, for a long time, considered to be a prototype for all other microbial retinal proteins [2]. With increasing interest in this class of proteins, driven by actual and potential applications of microbial rhodopsins such as channelrhodopsin in optogenetics [3], research in this field was revitalized and more retinal proteins were discovered in various organisms. Structure and function of these novel photoreceptors are far from being understood but many of their representatives display a photochemical behavior and mechanistic pattern of the retinal chromophore that differ substantially from BR [4].

We have recently reported on a member of a novel subfamily of histidine-kinase rhodopsins. Histidine kinase rhodopsin I (HKRI) found in the green alga *Chlamydomonas reinhardtii* [5] has been suggested to exert a function in adaptation of behavioral responses to the UV irradiation. HRK1 is a modular protein that comprises a photosensory rhodopsin, a histidine kinase, a response regulator and a putative guanylyl cyclase domain. The photosensor was found to exist in two parent states absorbing at 379 nm (Rh-UV) and 486 nm (Rh-Bl), which can be converted into each other by light of appropriate wavelengths. In this sense, HKR1 acts as a bimodal photoswitch. This contrasts the properties of other retinal proteins running through a unidirectional photoinduced reaction cycle. The color change associated with photoswitching of HKR1 is related to the protonation state of the Schiff base function that provides the linkage of the retinal chromophore with a Lys side chain of the protein. Resonance Raman (RR) spectroscopy has shown that in the Rh-UV state, the retinylidene chromophore is deprotonated and adopts a 13-*cis*,15-*anti* conformation as the M412 state of BR [2,5]. Photoconversion to Rh-Bl by UV irradiation, however, affords a mixture of 13-*trans*,15-*anti* and 13-*cis*,15-*syn* conformers, both carrying a protonated Schiff base as revealed by RR spectroscopy and retinal extraction experiments [5]. This structural heterogeneity of Rh-Bl is reminiscent of the dark-adapted form of BR, which results from the thermal chromophore isomerization of the light-adapted form [6,7].

We are therefore interested in exploring whether thermal retinal isomerization steps also take place in HKR1 and to analyze

Abbreviations: BR, bacteriorhodopsin; HKR1, histidine kinase rhodopsin 1; RSB, retinal Schiff base; RR, resonance Raman; Rh-Bl and Rh-UV, blue- and UV-absorbing form of the HKR1photosensor; Rh-Dark, initial dark state of the HRK1 photosensor

Author contributions: M. L., S. B., and A. K. carried out the experiments. P. He. and P. Hi. designed the experiments and wrote the manuscript. All authors contributed to the evaluation of the results.

* Corresponding authors. Fax: +49 30 2093 8520 (P. Hegemann), +49 30 31421122 (P. Hildebrandt).

E-mail addresses: hegemann@rz.hu-berlin.de (P. Hegemann), hildebrandt@chem.tu-berlin.de (P. Hildebrandt).

[1] Equal contribution to the work.

http://dx.doi.org/10.1016/j.febslet.2015.03.024
0014-5793/

their potential interference with photochemical isomerization routes. In this work we have employed UV–vis absorption and RR spectroscopy to analyze the various isomerization reactions from the cofactor-protein assembly to the transitions between Rh-Bl and Rh-UV.

2. Materials and methods

2.1. Protein expression

The used DNA-construct was a humanized *C. reinhardtii* HKR1 rhodopsin fragment (amino acids 1–265, accession number: AAQ16277) in a pPICz-vector including a C-terminal c-myc-tag and a 12x-histidine-tag. Heterologous protein expression was performed in the methylotrophic yeast *Pichia pastoris* strain 1168H and was induced by the addition of 2.5% methanol to the growth medium containing 5 μM *all-trans* retinal. Details of protein expression and purification procedures were described earlier [5]. The protein was solubilized in HEPES-buffer pH 7.4 with 0.03% dodecyl maltoside. For the analysis of Rh-Dark all expression and purification steps were performed under red dim light and under strict exclusion of any visible light source.

2.2. UV–vis absorption spectroscopy

Steady state absorption spectra were recorded in a Cary 300 Bio Spectrophotometer (Varian Inc., Darmstadt, Germany) at 20 °C with a resolution of 1.6 nm. The Rh-Dark sample was measured without light exposure except the spectrophotometer light (bandwidth: 1 nm, scan rate: 1454.546 nm/min). Formation of Rh-UV was induced by a 2 min illumination of either Rh-Dark or Rh-Blue with different light emitting diodes (LED, Nichia Corporation, Tokushima, Japan, 0.12 W), emitting at 470 nm (blue light), 530 nm (green light), or 590 nm (orange light). Rh-UV was converted to Rh-Bl by a 2 min illumination with a 0.11 W UV-LED (380 nm). Spectra were measured immediately after illumination and after a period of dark adaptation (minutes, hours and days) at room temperature. To ensure equal purification and buffer conditions of the three species, spectra were obtained from the same sample by the above described illumination procedures.

2.3. Resonance Raman spectroscopy

RR spectra were measured with 514 nm and 413 nm excitation of an Ar^+ and Kr^+ ion laser, respectively (Coherent, Santa Clara CA, U.S.A.). The Raman signals were detected in a backscattering configuration (180°) via a confocal LabRamHR spectrometer (Horiba, Villeneuve, France), equipped with a liquid-nitrogen cooled CCD detector. The resolution per pixel was between 0.4 cm^{-1}, corresponding to a spectral resolution of 1.2 cm^{-1}. Typical total accumulation times and laser powers at the sample were 1 h at ca. 1 mW, respectively. Low-temperature experiments were carried out with a Linkam cryostat (Linkam Scientific Instruments, Surrey, UJ), mounted on a computer controlled XY stage (OWIS GmbH, Germany). The cryostat was circularly moved through the laser focus to reduce unwanted photochemical processes. The samples were inserted into the cell under dimmed red light in order to avoid photoactivation before freezing. Further details of the set-up and the measurements were described elsewhere [5]. In all spectra shown in this work, the background was subtracted by a polynomial function. Band fitting and component analysis was carried out as described previously [8].

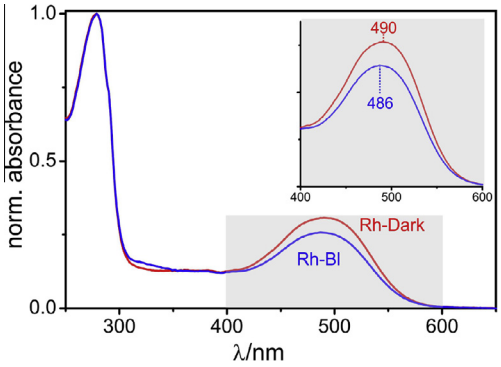

Fig. 1. UV–vis absorption spectra of Rh-Bl (blue) and Rh-Dark (red), measured in a HEPES buffer (pH 7.4) at 20 °C. Spectra were normalized to the absorbance maximum at 280 nm. The inset shows the enlarged spectra of Rh-Bl and Rh-Dark in the visible region. The respective absorption maxima are indicated.

3. Results and discussion

After purification under daylight conditions, the photosensor of HKR1 is largely in the Rh-UV state, which displays an absorption maximum at 379 nm with poorly resolved vibronic side bands (*vide infra*). In this state, the chromophore adopts a 13-*cis*,15-*anti* geometry with deprotonated Schiff base [5]. As concluded from a RR spectroscopic comparison, even structural details are very similar to the chromophore in the M412 state of BR although the absorption maximum of Rh-UV of HKR1 is shifted further to the UV by ca. 30 nm. Rh-UV can be reversibly converted to the Rh-Bl state that exhibits an absorption maximum at 486 nm (Fig. 1, blue trace), reflecting a mixture of both a 13-*trans*,15-*anti* and 13-*cis*,15-*syn* conformers, both carrying a protonated Schiff base [5].

3.1. The Rh-Dark state of HKR1

In case expression, protein-cofactor assembly with all-*trans* (13-*trans*,15-*anti*) retinal, and purification of HKR1 was carried out under strict red-light conditions, the absorption spectrum reveals no indication for Rh-UV but instead displays an absorption spectrum that is similar to that of Rh-Bl albeit not identical (Fig. 1). A careful inspection (Fig. 1, inset) shows a slight red-shift of the absorption maximum to 490 nm accompanied by an increase of the absorbance by nearly 20%. This initial state, denoted as Rh-Dark, is readily converted to Rh-UV upon irradiation with blue light but cannot be recovered photochemically since UV-irradiation affords Rh-Bl (*vide supra*). We thus conclude that the chromophore structure of the initially formed dark state Rh-Dark significantly differs from Rh-Bl.

3.2. Resonance Raman spectroscopic analysis of the Rh-Dark state

The irreversible light-induced conversion of Rh-Dark to Rh-UV makes it impossible to measure the RR spectra of Rh-Dark at ambient temperature. Since the photoinduced formation of Rh-UV is associated with thermal relaxation steps, one may reduce depletion of Rh-Dark and Rh-Bl in the exciting laser beam at sufficiently low temperature. This condition is in fact fulfilled at 80 K for Rh-Bl and the low-temperature RR spectrum can be directly compared with a RR spectrum obtained at ambient temperature in a dual-color experiment [5] (Fig. 2A and B). Although at ambient temperature additional UV-irradiation was used to continuously recover Rh-Bl from Rh-UV, a photostationary mixture between Rh-UV and Rh-Bl is established but only the spectrum of the latter species is resonantly enhanced at 514 nm. Compared to this spectrum, at low temperature only minor differences are noted which refer to

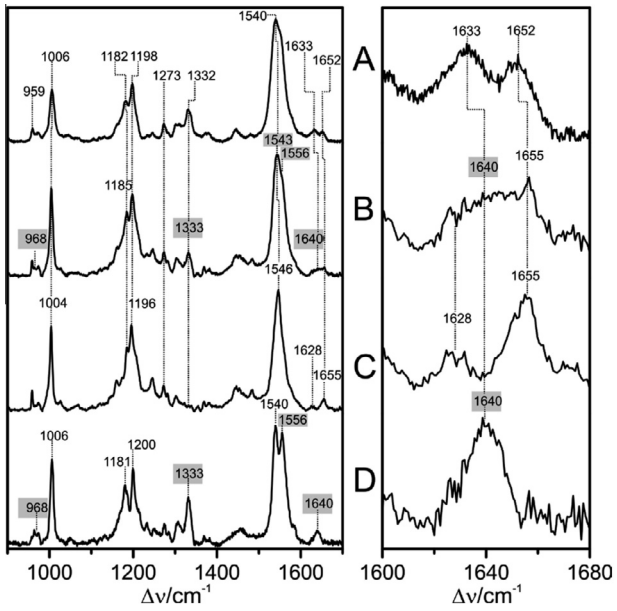

Fig. 2. RR spectra of HKR1 in different states. (A) Rh-Bl, measured in solution at ambient temperature in solution using a two-color technique to convert Rh-UV (formed during laser excitation) back to Rh-Bl (spectrum taken from Ref. [5]); (B) Rh-Bl, measured at 80 K; (C) Rh-Dark, measured at 80 K; (D) difference spectrum "B" minus "C" to afford the 13-*cis* component of Rh-Bl. All spectra were obtained with 514 nm excitation. The gray rectangles highlight some characteristic spectral differences between Rh-Bl and Rh-Dark. Further details are given in the text. All spectra were measured HEPES buffer at pH 7.4.

small frequency upshifts for a few bands and variations of the relative intensities as typically observed in RR experiments of chromoproteins [9]. There are no indications for further structural changes of the cofactor. Thus, we conclude that at 80 K Rh-Bl includes a similar mixture of protonated chromophores in the 13-*trans*,15-*anti* and 13-*cis*,15-*syn* configurations as at ambient temperature.

The RR spectrum of Rh-Dark measured at 80 K (Fig. 2C) differs from that of Rh-Bl (Fig. 2B) in some important details as highlighted by the gray-shaded rectangles. These differences include the 1333 cm^{-1} band (N–H ip) of Rh-Bl that disappeared in Rh-Dark, a change in the band profile of the C=C stretching modes at 1543 and 1556 cm^{-1}, and spectral changes in the region of the C=N stretching mode of the protonated retinal Schiff base (RSB) between 1620 and 1660 cm^{-1}. Here Rh-Bl, at ambient temperature, displays two separated peaks at 1652 and 1633 cm^{-1} (Fig. 2A) originating from the 13-*trans* and 13-*cis* isomer, respectively [5]. At 80 K, the temperature-dependent frequency shifts to ca. 1655 and 1640 cm^{-1} cause a strong overlap of both bands to afford a poorly structured envelope (Fig. 2B). The spectrum of Rh-Dark, however, only displays the band at 1655 cm^{-1} whereas there is no intensity at 1640 cm^{-1}. This observation suggests that Rh-Dark includes solely the 13-*trans*,15-*anti* conformer.

3.3. Resonance Raman spectra of the two isomers

The different chromophore compositions in Rh-Bl and Rh-Dark allow for generating the pure spectrum of the two isomers which was achieved *via* two approaches. First, the spectrum of Rh-Dark (Fig. 2C) was subtracted from that of Rh-Bl (Fig. 2B), using the 1333 cm^{-1} band as a reference. The resulting difference spectrum (Fig. 2D) does not display any artefacts such as negative peaks and thus is attributed to the spectrum of the 13-*cis* isomer in Rh-Bl. A second approach was employed on the basis of a band fitting analysis of the C=C stretching region between 1530 and 1570 cm^{-1} which includes two vibrational modes in each isomeric state. These two modes are due to the in-phase and out-of-phase C=C stretching of the polyene chain with the in-phase mode being at lower frequency than the out-of-phase mode in 13-*trans*,15-*anti* whereas in 13-*cis*,15-*syn* the order is reversed [10,11]. For the spectrum of Rh-Dark two Lorentzian functions are in fact sufficient to satisfactorily describe the peak envelope (Fig. 3A). Next, these two bands are used to generate a component spectrum for the 13-*trans* conformer. This component spectrum and two additional Lorentzian functions for the corresponding 13-*cis* conformer are then used to simulate the RR spectrum of Rh-Bl leading to two bands of comparable intensities that constitute the component spectrum of the 13-*cis* species (component analysis, see [8] and references therein). On the basis of the amplitudes of the two component spectra in the C=C stretching region (Fig. 3B), the weighting factor for the subtraction procedure "Rh-Bl minus Rh-Dark" can be now calculated rather than estimated by visual inspection as in the first approach. Altogether, both subtraction procedures afford essentially the same spectrum of the 13-*cis* conformer.

In general, the pure spectra of the 13-*trans* and 13-*cis* conformers are very similar to the respective component spectra of the 13-*trans*,15-*anti* and 13-*cis*,15-*syn* counterparts in the light- and dark-adapted forms of BR [11,12], confirming the previous assignment for Schiff base configurations [5]. For instance, the 1161 cm^{-1} band in the spectrum of Rh-Dark is a marker band for the 13-*trans*,15-*anti* configuration (Fig. 3D) [10], whereas the prominent bands at 1181 and 1200 cm^{-1} of the 13-*cis* species (difference spectrum in Fig. 3E) are considered to be a characteristic signature for the 13-*cis*,15-*syn* configuration [11]. Also the splitting between the two C=C stretching modes (ca. 20 cm^{-1}; Fig. 3B) is the same as for the 13-*cis*,15-*syn* isomer of dark-adapted BR and distinctly larger than for the 13-*cis*,15-*anti* form in the L550 intermediate of BR [13]. The main spectral difference compared to BR refers to the positions of the in-phase C=C stretching modes which are higher in the HKR1 isomers (1545.2 and 1556.7 cm^{-1}; Fig. 2A and C) compared to the BR counterparts [10,11]. This can be readily understood in terms of the blue-shifted absorption maxima that reflect a lower degree of π-electron delocalization, corresponding to a weakening of the C=C stretching force constants in the 13-*trans* and 13-*cis* conformers of HKR1 [14]. This inverse correlation between the absorption maxima and the frequencies of in-phase C=C stretching modes further suggests a red-shifted absorption maximum of the 13-*trans* conformer compared to 13-*cis* species. This conclusion is consistent with the absorption spectrum of Rh-Dark (only 13-*trans*) that exhibits a maximum at slightly longer wavelengths than Rh-Bl (13-*trans*/13-*cis*) (Fig. 1).

3.4. Photochemical and thermal chromophore isomerizations

To explore the photochemical pathways of the conversion between Rh-Bl and Rh-UV, we have employed different irradiation wavelengths at the short (blue LED) and long wavelength side (green and orange LED) of the absorption band of Rh-Bl. Upon blue irradiation of Rh-Bl, the resultant photoproduct displayed an absorption spectrum similar to that of the UV-absorbing state that prevails under daylight conditions (Fig. 4, black trace). However, excitation with green or orange light yielded a different state characterized by an increased intensity at 396 nm at the expense of the shoulder at 365 nm (Fig. 4, magenta trace). Evidently, the spectral differences reflect different isomeric compositions and we denote the corresponding states as Rh-UV1 (black trace) and Rh-UV2 (magenta trace). In contrast to Rh-Bl, irradiation of Rh-Dark led to the same Rh-UV1 state, regardless of the irradiation wavelength. Both Rh-UV1 and Rh-UV2 were readily converted back to Rh-Bl by UV light, independent of preceding irradiation sequences.

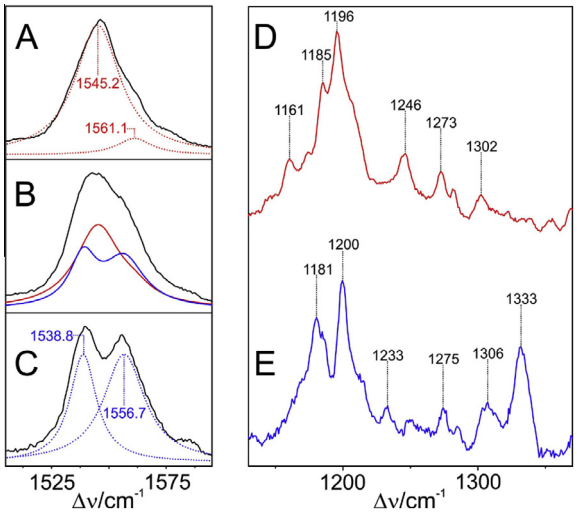

Fig. 3. RR spectra of HKR1 in the C=C stretching region (left panel) and the fingerprint region (right panel). The left panel shows the spectrum of (A) Rh-Dark including only the 13-*trans*,15-*anti* conformer, (B) Rh-Bl including both the 13-*trans*,15-*anti* and 13-*cis*,15-*syn* conformer, and (C) the difference spectrum ("B" minus "A"), showing only the 13-*cis*,15-*syn* conformer. The red and blue lines represent the fitted bands (dotted)/component spectra (solid) of the 13-*trans* and 13-*cis* species, respectively. Details of the fitting procedure are given in the text. The right panel shows the pure spectra of (D) the 13-*trans*,15-*anti* conformer (corresponding to Rh-Dark) and (E) the 13-*cis*,15-*syn* conformer (obtained by subtraction "Rh-Bl" minus "Rh-Dark", as described in the text). All spectra were measured HEPES buffer at pH 7.4 with 514 nm excitation.

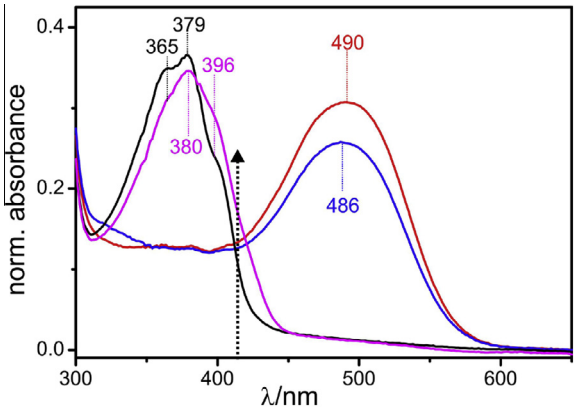

Fig. 4. UV–vis absorption spectra of Rh-UV1 (black), Rh-UV2 (magenta), Rh-Bl (rblue), and Rh-Dark (red), measured in HEPES buffer (pH 7.4) at 20 °C. The spectra of Rh-UV1 and Rh-UV2 were obtained after irradiation of Rh-Bl with blue and green light, respectively. The vertical dotted arrow indicates the position of the 413-nm laser line in the RR experiment.

To identify the underlying isomeric differences, the Rh-UV1 and Rh-UV2 states were studied by RR spectroscopy at 80 K using 413 nm excitation (1 mW). However, in each case essentially the same spectra were obtained. These spectra agree very well with that reported previously which was attributed to a 13-*cis*,15-*anti* configuration of a deprotonated RSB [5]. In fact, besides a contribution of the Rh-Bl state, the absorption spectra measured immediately after the RR experiments included only the Rh-UV1 state. These findings imply that at 80 K the 413-nm excitation line causes the photoconversion of Rh-UV2 to Rh-UV1 during the RR experiment. Such a photochemical Rh-UV2 → Rh-UV1 conversion was also observed with blue irradiation at ambient temperature due to the higher absorption of Rh-UV2 above 400 nm (Fig. 4).

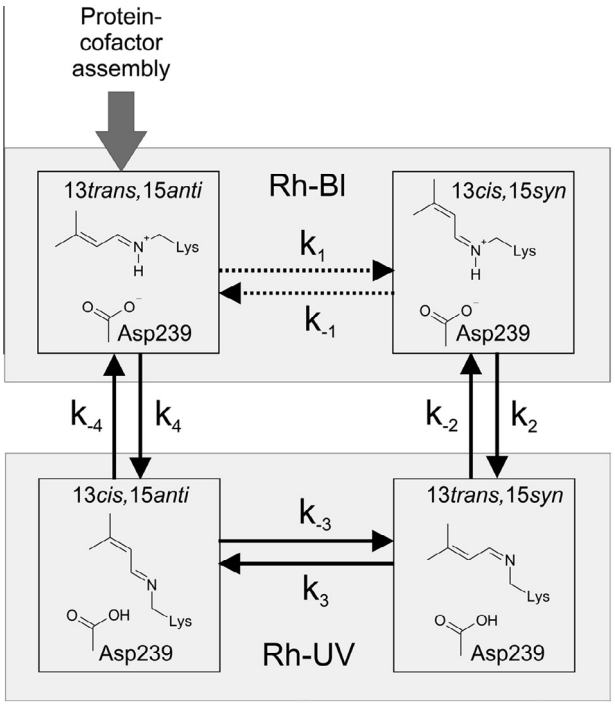

Fig. 5. Reaction scheme for the photoinduced transformations between the 13-*trans* and 13-*cis* conformers in the Rh-Bl and Rh-UV state. The Rh-Dark state, formed upon cofactor-protein assembly in the dark, exclusively contains the protonated RSB in the 13-*trans*,15-*anti* configuration. The Rh-UV1 state only includes the deprotonated RSB in the 13-*cis*,15-*anti* configuration whereas the Rh-UV2 state also includes a contribution of the deprotonated 13-*trans*,15-*syn* RSB. The black solid arrows indicate photoinduced reactions as derived from the spectroscopic data whereas the dotted arrows represent possible albeit not proven photoreactions.

These light-induced reactions can readily be rationalized starting with the photoinduced transition of Rh-Dark to Rh-UV1 which corresponds simply to the C(13)=C(14) double bond isomerization from the 13-*trans* to the 13-*cis* configuration, accompanied by the deprotonation of the Schiff base which remains in the *anti* configuration (Fig. 5, reaction k_4). In addition to the 13-*trans*, 15-*anti* isomer undergoing the C(13)=C(14) photoisomerization, Rh-Bl also includes a 13-*cis*,15-*syn* configuration which is photoconverted as well to a deprotonated RSB isomer. It is reasonable to assume that also in this case the primary event is the C(13)=C(14) double bond isomerization resulting in 13-*trans*, 15-*syn* deprotonated RSB (Fig. 5, reaction k_2). Using blue LED or 413-nm laser irradiation (RR experiment), this isomer is then, after absorption of second photon, further converted into the 13-*cis*,15-*anti* deprotonated RSB (Rh-UV1), corresponding to the simultaneous rotation around the C(13)=C(14) and C(15)=N double bonds (Fig. 5, reaction k_3). Evidently, the efficiency of this transition decreases with increasing irradiation wavelength such that with green or orange light a fraction of the chromophores remains in the deprotonated 13-*trans*,15-*syn* RSB corresponding to Rh-UV2. Thus, the absorption spectrum of Rh-UV2 is attributed to a mixture of deprotonated 13-*trans*,15-*syn* and 13-*cis*,15-*anti* RSB (Fig. 5).

The photochemical back conversion of Rh-UV1 and Rh-UV2 always leads to the same Rh-Bl state. For Rh-UV2, this transition solely comprises photoisomerization around the C(13)=C(14) double bond and subsequent reprotonation of the RSB, resulting in a mixture between protonated 13-*trans*,15-*anti* and 13-*cis*,15-*syn* RSB isomers (reactions k_{-4} and k_{-2}). For the photoconversion of Rh-UV1 including solely the deprotonated 13-*cis*,15-*anti* RSB

isomer, the photoinduced reaction k_{-4} yields only the protonated 13-*trans*,15-*anti* component of Rh-Bl. To account for formation of the protonated 13-*cis*,15-*syn* isomer of Rh-Bl upon UV-light irradiation, we propose that a fraction of the Rh-UV1 state first undergoes a simultaneous photoisomerization around the C(13)=C(14) and C(15)=N double bonds to afford the deprotonated 13-*trans*,15-*syn* RSB (k_{-3}), followed by the 13-*trans* → 13-*cis* double bond isomerization and subsequent Schiff base protonation (k_{-2}). The alternative photochemical route *via* reaction k_{-4} and k_1 is less likely due to the very low absorbance of the protonated 13-*trans*,15-*anti* isomer of Rh-Bl in the UV. Whether photochemical transitions between the Rh-Bl isomers (k_1, k_{-1}) are possible with blue light irradiation, cannot be decided on the basis of the present experiments. On the other hand, we can safely rule out a coupling of photoisomerizations of the *15-anti* isomers (k_4 and k_{-4}) with rapid thermal 15-*anti*/15-*syn* isomerizations as suggested previously [5]. Dark conversion of Rh-Dark to Rh-Bl, if it takes place at all, must proceed on the time scale of days such that the underlying thermal dark state isomerization of the 13-*trans*,15-*anti* to the 13-*cis*,15-*syn* protonated RSB and its corresponding back reaction cannot account for the complete light-induced conversion of Rh-UV1 into Rh-Bl within a few milliseconds. In addition, a rapid thermal isomerization of the deprotonated RSB isomers can be discarded since the UV–vis absorption spectra of Rh-UV1 and Rh-UV2 do not change at least within 1 h.

Thus, in summary, the conversion between the four RSBs in Rh-UV and Rh-Bl proceed via multiple photoisomerization steps include rotations around one double bond (13-*trans*/13-*cis*) of protonated RSB isomers (Rh-Bl) and simultaneous rotations around two double bonds (13-*trans*/13-*cis* and 15-*anti*/15-*syn*) of deprotonated RSB isomers (Rh-UV).

Finally, we like to comment on the nature of the Rh-Dark state. There is no indication that, once Rh-UV or Rh-Bl is formed, this state can be ever recovered by keeping the sample in the dark even for days. We thus conclude that Rh-Dark represents the initial cofactor-protein complex formed after assembly of the apoprotein with all-*trans* retinal. Thus, Rh-Dark is likely to be the last precursor in the maturation of the fully functional HKR1.

Acknowledgements

The work was supported by the German Research Foundation, DFG (Sfb1078 projects B6, B1 and the Cluster of Excellence *Unifying Concepts of Catalysis*).

References

[1] Briggs, W.R. and Spudich, J.L., Eds., (2005). Handbook of Photosensory Receptors, Wiley-VCH, Weinheim/Germany.
[2] Lanyi, J.K. (2004) Bacteriorhodopsin. Annu. Rev. Physiol. 66, 665–688.
[3] Gunaydin, L.A., Yizhar, O., Berndt, A., Sohal, V.S., Deisseroth, K. and Hegemann, P. (2010) Ultrafast optogenetic control. Nat. Neurosci. 13, 387–392.
[4] Ernst, O.P., Lodowski, D.T., Elstner, M., Hegemann, P., Brown, L.S. and Kandori, H. (2014) Microbial and animal rhodopsins: structures, functions, and molecular mechanisms. Chem. Rev. 114, 126–163.
[5] Luck, M., Mathes, T., Bruun, S., Fudim, R., Hagedorn, R., Tran Nguyen, T.M., Kateriya, S., Kennis, J.T., Hildebrandt, P. and Hegemann, P. (2012) A photochromic histidine kinase rhodopsin (HKR1) that is bimodally switched by ultraviolet and blue light. J. Biol. Chem. 287, 40083–40090.
[6] Sperling, W., Carl, P., Rafferty, C.N. and Dencher, N.A. (1977) Photochemistry and dark equilibrium of retinal isomers and bacteriorhodopsin isomers. Biophys. Struct. Mech. 3, 79–94.
[7] Kalisky, O., Goldschmidt, C.R. and Ottolenghi, M. (1977) On the photocycle and light adaptation of dark-adapted bacteriorhodopsin. Biophys. J. 19, 185–189.
[8] Ly, H.K., Utesch, T., Diaz-Moreno, I., Garcia-Heredia, J.M., De La Rosa, M.A. and Hildebrandt, P. (2012) Perturbation of the redox site structure of cytochrome *c* variants upon tyrosine nitration. J. Phys. Chem. B 116, 5694–5702.
[9] Cartling, B. (1983) Intermediate and stable redox states of cytochrome *c* studied by low temperature resonance Raman spectroscopy. Biophys. J. 43, 191–205.
[10] Smith, S.O., Braiman, M.S., Myers, A., Pardoen, J.A., Courtin, J.M.L., Winkel, C., Lugtenburg, J. and Mathies, R.A. (1987) Vibrational analysis of the all-*trans* retinal chromophore in light-adapted bacteriorhodopsin. J. Am. Chem. Soc. 109, 3108–3125.
[11] Smith, S.O., Pardoen, J.A., Lugtenburg, J. and Mathies, R.A. (1987) Vibrational analysis of the 13-*cis* retinal chromophore in dark-adapted bacteriorhodopsin. J. Phys. Chem. 91, 804–819.
[12] Alshuth, T. and Stockburger, M. (1981) Structural changes in the retinal chromophore of bacteriorhodopsin studied by resonance Raman spectroscopy. Ber. Bunsenges. Phys. Chem. 85, 484–489.
[13] Smith, S.O., Lugtenburg, J. and Mathies, R.A. (1985) Determination of retinal chromophore structure in bacteriorhodopsin with resonance Raman spectroscopy. J. Membr. Biol. 85, 95–109.
[14] Heyde, M.E., Gill, D., Kilponen, R.G. and Rimai, L. (1971) Raman spectra of Schiff bases of retinal (models of visual photoreceptors). J. Am. Chem. Soc. 93, 6776–6780.